

Pion-mass dependence of the nucleon-nucleon interaction in the 3S_1 - 3D_1 coupled channel

Qian-Qian Bai and Chun-Xuan Wang
School of Physics, Beihang University, Beijing 102206, China

Yang Xiao
*School of Physics, Beihang University, Beijing 102206, China and
Université Paris-Saclay, CNRS/IN2P3, IJCLab, 91405 Orsay, France*

Li-Sheng Geng*
*School of Physics, Beihang University, Beijing 102206, China.
Beijing Key Laboratory of Advanced Nuclear Materials and Physics, Beihang University, Beijing, 102206, China and
School of Physics and Microelectronics, Zhengzhou University, Zhengzhou, Henan 450001, China*
(Dated: May 20, 2021)

In this work, we explore the predictive power of the recently proposed covariant chiral nuclear force. In particular, we focus on the 3S_1 - 3D_1 coupled channel and show that it is capable to predict the 3D_1 phase shifts and mixing angle ε_1 by fitting to the 3S_1 phase shifts, or predict the 3S_1 phase shifts by fitting to the 3D_1 phase shifts and mixing angle ε_1 . For the physical nucleon-nucleon phase shifts, one can achieve a reasonably good description up to $T_{\text{lab.}} \approx 100$ MeV. Qualitative descriptions can be achieved up to even higher energies. On the other hand, for the lattice QCD nucleon-nucleon phase shifts obtained with $M_\pi = 469$ MeV, the energy range for which a decent description can be achieved is much reduced, to only $T_{\text{lab.}} \approx 10$ MeV. In addition, we show that with one more low energy constant, particularly, one for the mixing angle, the next-to-leading order heavy baryon chiral nuclear force can describe the lattice QCD data up to $T_{\text{lab.}} \approx 40$ MeV, but the description of the physical nucleon-nucleon phase shifts is of similar quality to the leading order covariant chiral nuclear force. The present study is relevant to a better understanding of the lattice QCD nucleon-nucleon force or more general baryon-baryon interactions.

PACS numbers:

I. INTRODUCTION

Lattice QCD simulations have become an indispensable tool to explore the non-perturbative baryon-baryon interactions, in particular, hyperon-nucleon and hyperon-hyperon interactions [1–6], which have so far remain difficult to be studied experimentally. Nonetheless, lattice QCD simulations of coupled channel baryon-baryon interactions are very challenging as well (see, e.g., Refs. [7, 8]). In this sense, reliable theoretical studies of lattice QCD simulations are in urgent need, particularly for those simulations performed for unphysical pion masses, which remain unconstrained. One of such theoretical tools is chiral perturbation theory [9–11](see Ref. [12] for a review) and the resulting chiral nuclear forces [13–18]. It should be noted that the conventional chiral nuclear forces are based on the heavy baryon (HB) version of chiral perturbation theory [19, 20]. In recent years, it has been proposed that one can build a covariant version of chiral nuclear forces with the covariant baryon chiral perturbation theory [21, 22]. Such proposals have been explored mainly by two groups, the Bochum group [23–25] and the BUAA group [26–34].

In addition to being covariant, the newly proposed scheme has another interesting feature, i.e., some low energy constants contribute to different partial wave phase shifts. This is

in contrast with the conventional chiral nuclear force, where a single LEC only contributes to a particular partial wave. The particular feature raises two intriguing questions: 1) whether such correlations are physical and supported by data; 2) how they can be utilized to better understand lattice QCD simulations for unphysical pion masses or baryon-baryon interactions where there are little or no constraints. It is the main purpose of the present work to address these two questions.

To address the first question, we turn to the physical nucleon-nucleon phase shifts, which have been measured very precisely. We show that it is possible to fix the unknown LECs by fitting to either δ_{3S_1} and then predict δ_{3D_1} and ε_1 up to $T_{\text{lab.}} \approx 100$ MeV. Similarly, we can also fit to δ_{3D_1} and ε_1 and predict δ_{3S_1} . These demonstrate that the correlation contained in the covariant chiral EFT is indeed correct.

To address the second question, we apply the same approach to study the lattice QCD nucleon-nucleon phase shifts for $m_\pi = 469$ MeV [35]. Although the covariant approach works more or less fine, but the largest $T_{\text{lab.}}$ for which a reasonable description can be achieved is reduced to about 10 MeV. This seems to indicate that for some unknown reasons, the application region of the covariant chiral EFT for unphysical pion masses is much smaller.

To check whether this is particular to the covariant chiral nuclear force, we turn to the next-to-leading order HB chiral effective field theory, because in this case, only one more LEC is needed [36], while in the covariant case, more LECs are needed and therefore they cannot be properly determined by the limited lattice QCD data [35]. We show that the NLO HB chiral nuclear force can describe the lattice QCD data up to

*Electronic address: lisheng.geng@buaa.edu.cn

$T_{\text{lab.}} \approx 40$ MeV, but the description of the physical nucleon-nucleon phase shifts remain similar to the leading order covariant ChEFT. We can trace the improvement to the decoupling of the different partial waves and to the fact that one independent LEC appears for the mixing angle.

This work is organized as follows. In Sec.II, we briefly introduce the leading order covariant ChEFT and the next-to-leading order HB ChEFT, with particular emphasis on the description of light quark mass dependence. In Sec.III, we study the predictive power of the covariant ChEFT for both the physical nucleon-nucleon phase shifts and the lattice QCD nucleon-nucleon phase shifts. Then, we explore how the next-to-leading order HB chiral nuclear force can describe the lattice QCD data. A short summary and outlook is given in Sec.IV.

II. THEORETICAL FRAMEWORK

The ChEFT we employ in the present work is described in detail in Refs. [26, 29, 33]. Here we only provide a concise introduction and relevant formulation needed for studying the light quark mass dependence of the NN interaction.

At leading order, the covariant chiral potential in the pion-full version can be written as.

$$V_{LO} = V_{CT} + V_{OPE} \quad (1)$$

where V_{CT} represents contact contributions and V_{OPE} denotes one-pion exchanges. The contact contributions are described by four covariant four-fermion contact terms without derivatives [29], namely,

$$\begin{aligned} V_{CT} = & C_S [\bar{u}(\mathbf{p}', s'_1) u(\mathbf{p}, s_1)] [\bar{u}(-\mathbf{p}', s'_2) u(-\mathbf{p}, s_2)] \\ & + C_V [\bar{u}(\mathbf{p}', s'_1) \gamma_\mu u(\mathbf{p}, s_1)] [\bar{u}(-\mathbf{p}', s'_2) \gamma^\mu u(-\mathbf{p}, s_2)] \quad (2) \\ & + C_{AV} [\bar{u}(\mathbf{p}', s'_1) \gamma_5 \gamma_\mu u(\mathbf{p}, s_1)] [\bar{u}(-\mathbf{p}', s'_2) \gamma_5 \gamma^\mu u(-\mathbf{p}, s_2)] \\ & + C_T [\bar{u}(\mathbf{p}', s'_1) \sigma_{\mu\nu} u(\mathbf{p}, s_1)] [\bar{u}(-\mathbf{p}', s'_2) \sigma^{\mu\nu} u(-\mathbf{p}, s_2)], \end{aligned}$$

where \mathbf{p} and \mathbf{p}' are initial and final three momentum, $s_1(s'_1)$, $s_2(s'_2)$ are spin projections, $C_{S,V,AV,T}$ are LECs, and $u(\bar{u})$ are Dirac spinors,

$$u(\mathbf{p}, s) = N_P \begin{pmatrix} 1 \\ \boldsymbol{\sigma} \cdot \mathbf{p} \\ E_P + M \end{pmatrix} \chi_S, \quad N_P = \sqrt{\frac{E_P + M}{2M}} \quad (3)$$

with χ_S being the Pauli spinor and $E_P(M)$ being the nucleon energy (mass). The one-pion-exchange potential in momentum space reads

$$\begin{aligned} V_{OPE}(\mathbf{p}', \mathbf{p}) = & -\left(g_A^2/4f_\pi^2\right) \times [\bar{u}(\mathbf{p}', s'_1) \boldsymbol{\tau}_1 \gamma^\mu \gamma_5 q_\mu u(\mathbf{p}, s_1)] \\ & \times \frac{\bar{u}(-\mathbf{p}', s'_2) \boldsymbol{\tau}_2 \gamma^\mu \gamma_5 q_\mu u(-\mathbf{p}, s_2)}{(E_{p'} - E_p)^2 - (\mathbf{p}' - \mathbf{p})^2 - m_\pi^2}, \quad (4) \end{aligned}$$

where m_π is the pion mass, $\tau_{1,2}$ are the isospin matrices, $g_A = 1.26$, and $f_\pi = 92.4$ MeV. Note that the leading order covariant potentials already contain all the six spin operators needed to describe nucleon-nucleon scattering.

Up to the next-to-leading order, the conventional (non-relativistic) chiral potential contains three terms [36], i.e.,

$$V_{NLO} = V_{CT} + V_{OPE} + V_{TPE}, \quad (5)$$

where the contact term, the one-pion exchange term, and the two-pion exchange term read, respectively,

$$V_{CT} = V_{CT}^{(0)} + V_{CT}^{(2)}, \quad (6)$$

$$V_{CT}^{(0)} = C_S + C_T \vec{\sigma}_1 \cdot \vec{\sigma}_2, \quad (7)$$

$$\begin{aligned} V_{CT}^{(2)} = & C_1 q^2 + C_2 k^2 + (C_3 q^2 + C_4 k^2) (\vec{\sigma}_1 \cdot \vec{\sigma}_2) \\ & + \frac{i}{2} C_5 (\vec{\sigma}_1 + \vec{\sigma}_2) \cdot (\vec{k} \times \vec{q}) + C_6 (\vec{q} \cdot \vec{\sigma}_1) (\vec{q} \cdot \vec{\sigma}_2) \\ & + C_7 (\vec{k} \cdot \vec{\sigma}_1) (\vec{k} \cdot \vec{\sigma}_2), \quad (8) \end{aligned}$$

$$V_{OPE} = -\frac{g_A^2}{4F_\pi^2} \frac{\vec{\sigma}_1 \cdot \vec{q} \vec{\sigma}_2 \cdot \vec{q}}{q^2 + m_\pi^2}, \quad (9)$$

$$\begin{aligned} V_{TPE} = & V_C + \boldsymbol{\tau}_1 \cdot \boldsymbol{\tau}_2 W_C \\ & + [V_S + \boldsymbol{\tau}_1 \cdot \boldsymbol{\tau}_2 W_S] \vec{\sigma}_1 \cdot \vec{\sigma}_2 \\ & + [V_T + \boldsymbol{\tau}_1 \cdot \boldsymbol{\tau}_2 W_T] \vec{\sigma}_1 \cdot \vec{q} \vec{\sigma}_2 \cdot \vec{q} \\ & + [V_{LS} + \boldsymbol{\tau}_1 \cdot \boldsymbol{\tau}_2 W_{LS}] i(\vec{\sigma}_1 + \vec{\sigma}_2) \cdot (\vec{q} \times \vec{k}), \quad (10) \end{aligned}$$

where $\vec{k} = (\vec{p} + \vec{p}')/2$, $\boldsymbol{\tau}_i$ denote the isospin Pauli matrices associated with the nucleon i , while $V_{C,S,T,LS}$ and $W_{C,S,T,LS}$ are scalar functions which depend on the nucleon momenta. The order- Q^2 contributions take the following form

$$\begin{aligned} W_C^{(2)} = & -\frac{L(q)}{384\pi^2 F_\pi^4} [4m_\pi^2 (5g_A^4 - 4g_A^2 - 1) \\ & + q^2 (23g_A^4 - 10g_A^2 - 1) + \frac{48g_A^4 m_\pi^4}{(4m_\pi^2 + q^2)}], \quad (11) \end{aligned}$$

$$V_T^{(2)} = -\frac{1}{q^2} V_S^{(2)} = -\frac{3g_A^4}{64\pi^2 F_\pi^4} L(q), \quad (12)$$

$$V_C^{(2)} = V_{LS}^{(2)} = W_S^{(2)} = W_T^{(2)} = W_{LS}^{(2)} = 0. \quad (13)$$

The loop function $L(q)$ is defined in dimensional regularization (DR) as

$$L(q) = \frac{\sqrt{4m_\pi^2 + q^2}}{q} \text{In} \frac{\sqrt{4m_\pi^2 + q^2} + q}{2m_\pi}. \quad (14)$$

The contact potentials can be projected into different partial waves in the $|LSJ\rangle$ basis. In the present work, we are only

interested in the 3S_1 - 3D_1 coupled channel. In the covariant ChEFT, the corresponding partial wave potentials read

$$V_{3S_1} = \frac{\xi_N}{9} \left[C_{3S_1} (9 + R_p^2 R_{p'}^2) + \hat{C}_{3S_1} (R_p^2 + R_{p'}^2) \right], \quad (15)$$

$$V_{3D_1} = \frac{8\xi_N}{9} C_{3S_1} R_p^2 R_{p'}^2, \quad (16)$$

$$V_{3S_1-3D_1} = \frac{2\sqrt{2}\xi_N}{9} \left[C_{3S_1} R_p^2 R_{p'}^2 + \hat{C}_{3S_1} R_p^2 \right], \quad (17)$$

$$V_{3D_1-3S_1} = \frac{2\sqrt{2}\xi_N}{9} \left[C_{3S_1} R_p^2 R_{p'}^2 + \hat{C}_{3S_1} R_{p'}^2 \right], \quad (18)$$

where $\xi_N = 4\pi N_p^2 N_{p'}^2$, $R_p = |\mathbf{p}|/(E_p + M)$, and $R_{p'} = |\mathbf{p}'|/(E_{p'} + M)$.

In the conventional ChEFT up to NLO, the 3S_1 - 3D_1 coupled channel potentials read

$$V_{3S_1} = \tilde{C}_{3S_1} + C_{3S_1} (\mathbf{p}^2 + \mathbf{p}'^2), \quad (19)$$

$$V_{3S_1-3D_1} = C_{3DS_1} \mathbf{p}^2, \quad (20)$$

$$V_{3D_1-3S_1} = C_{3DS_1} \mathbf{p}'^2, \quad (21)$$

where C_{3S_1} , \tilde{C}_{3S_1} , and C_{3DS_1} are linear combinations of C_S , C_T , and $C_{1,2,3,4,5,6,7}$, which are not relevant to our purpose here. We note that there are no LECs contributing to V_{3D_1} up to NLO. As a result, only the OPE and TPE contribute to δ_{3D_1} .

To study pion mass dependent lattice QCD data, in the covariant ChEFT, following Ref. [32], we add a pion-mass dependent term in the 3S_1 potential but keep the momentum expansion at the leading order, similar to, e.g., Ref. [37]. The resulting LECs then read, explicitly,

$$C_{3S_1} \rightarrow C_{3S_1} + C_{3S_1}^\pi m_\pi^2, \quad (22)$$

$$\hat{C}_{3S_1} \rightarrow \hat{C}_{3S_1} + \hat{C}_{3S_1}^\pi m_\pi^2. \quad (23)$$

Similarly, in the NLO conventional ChEFT, one also adds one pion mass dependent term

$$\tilde{C}_{3S_1} \rightarrow \tilde{C}_{3S_1} + C_{3S_1}^\pi m_\pi^2, \quad (24)$$

$$C_{3S_1} \rightarrow C_{3S_1}, \quad (25)$$

$$C_{3DS_1} \rightarrow C_{3DS_1}. \quad (26)$$

Comparing the leading order covariant ChEFT and the next-to-leading order HB ChEFT, it is clear that one more LEC is needed in the latter, i.e., C_{3DS_1} . In the covariant ChEFT, however, there are only two LECs for the 3S_1 - 3D_1 coupled channel. As a result, one can anticipate that the mixing angle can be better described in the latter.

III. RESULTS AND DISCUSSIONS

In this section, we first demonstrate the predictive power of the covariant ChEFT, in particular, its ability to connect δ_{3S_1} , δ_{3D_1} , and ε_1 , both for physical M_π and $M_\pi = 469$ MeV. Then to confirm the observation that the lattice QCD data can only be described up to $T_{\text{lab.}} \approx 10$ MeV, we turn to the next to leading order HBChEFT, where there is no correlation between the LECs for different partial waves, and therefore we expect that the lattice QCD simulations can be better described¹. We show that even in such a case the lattice QCD data can only be qualitatively described up to $T_{\text{lab.}} \approx 40$ MeV. The energy range for which the NLO HBChPT works is still much reduced compared to the physical nucleon-nucleon phase shifts.

TABLE I: Values of the LECs of the best fit to the Nijmegen δ_{3S_1} . The LECs in the first column are obtained by fitting to four experimental data up to $T_{\text{max}} = 100$ MeV and those in the second column by fitting to five experimental data up to $T_{\text{max}} = 150$ MeV.

C_{3S_1} [10^{-2} MeV $^{-2}$]	\hat{C}_{3S_1} [10^{-2} MeV $^{-2}$]	Λ [MeV]
-0.141	-0.686	905
-0.126	-0.603	920

A. Covariant ChEFT

First, we fix the two LECs C_{3S_1} and \hat{C}_{3S_1} and the cutoff by fitting to δ_{3S_1} for $T_{\text{lab.}} < 100$ and 150 MeV, respectively. The resulting LECs and phase shifts are shown in Table I and the left panel of Fig. 1. With the same LECs and cutoff, we predict δ_{3D_1} and ε_1 , which are shown in the middle and right panels of Fig. 1. Two things are noteworthy. First, the 3S_1 phase shifts can be described quite well, regardless of the T_{max} fitted. Second, the predicted δ_{3D_1} and ε_1 are in reasonable agreement with the data, particularly the former. The description of the mixing angle is not very satisfactory, but the qualitative feature is produced.

Next we fix the two LECs C_{3S_1} and \hat{C}_{3S_1} and the cutoff by fitting to δ_{3D_1} and ε_1 . Then we predict δ_{3S_1} . The corresponding LECs and phase shifts are shown in Table II and Fig. 2. We note that the predicted δ_{3S_1} are also in reasonable agreement with data. Contrary to the previous case, now one can better describe both δ_{3D_1} and ε_1 , particularly the latter. This is because the mixing angle is much small in magnitude compared to δ_{3S_1} , while in our fitting, we assigned the same weights to δ_{3S_1} , δ_{3D_1} , and ε_1 .

We stress that in both cases the correlation implicitly contained in the contact terms of the covariant framework is

¹ It has been shown that in Ref. [26] the LO covariant ChEFT can describe the $J = 0, 1$ nucleon-nucleon partial waves at a level similar to the NLO HB ChPT, although with a smaller number of LECs.

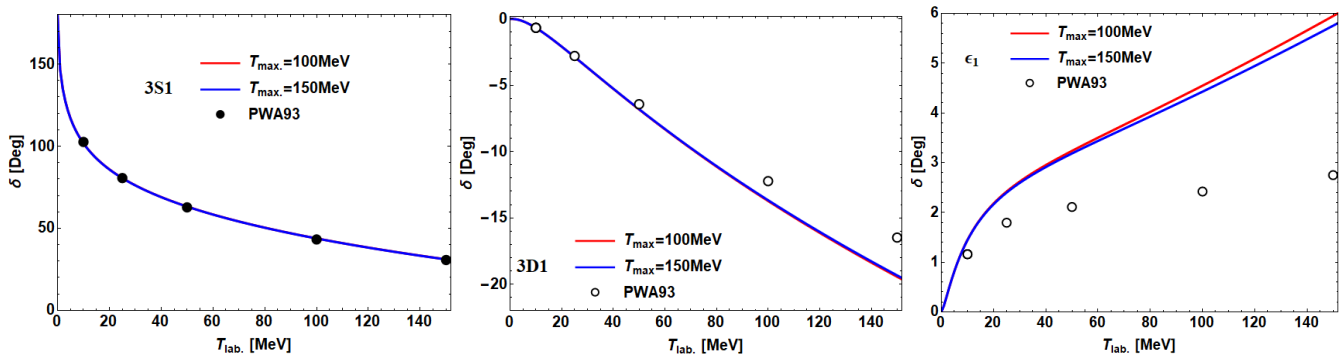


FIG. 1: Fitting to δ_{3S1} and predicting δ_{3D1} and ϵ_1 by the covariant ChEFT. Solid circles denote the data fitted and empty ones denote those not fitted.

supported. Similar correlations have been noticed in the strangeness $S = -3/-4$ baryon-baryon [34] as well as the $\Lambda_c N$ systems [38, 39], although for unphysical pion masses.

TABLE II: Same as Table II, but fitted to δ_{3D1} and ϵ_1 .

$C_{3S1} [10^{-4} \text{ MeV}^{-2}]$	$\hat{C}_{3S1} [10^{-2} \text{ MeV}^{-2}]$	$\Lambda [\text{MeV}]$
0.268	0.123	1135
0.259	0.122	1130

Now we turn to the lattice QCD nucleon-nucleon phase shifts obtained for $M_\pi = 469$ MeV, which have been studied in Refs. [32, 40]. First, we notice that the energy range for which a simultaneous description of δ_{3S1} , δ_{3D1} , and ϵ_1 can be achieved is much reduced [32]. Therefore, in the following, we check the largest kinetic energy up to which a reasonable description can be achieved. We again explore the two strategies adopted for studying the physical nucleon-nucleon phase shifts.

First, we fit to δ_{3S1} up to $T_{\text{lab.}} \approx 6$ and 12 MeV, and predict δ_{3D1} and ϵ_1 . The corresponding LECs² are listed in Table III and phase shifts given in Fig. 3. Clearly, although the central values of δ_{3S1} are fitted quite well, the predicted δ_{3D1} and ϵ_1 are a bit off. Two features of the lattice QCD data are responsible for this failure. First, the lattice QCD δ_{3D1} in the energy range studied are practically zero. Second, the mixing angle ϵ_1 are very small as well. As a matter of fact, as noted in Ref. [32], the mixing angle ϵ_1 for $M_\pi = 469$ MeV is similar to that for $M_\pi = 138$ MeV, exhibiting little light quark mass dependence.

Considering that the uncertainties of δ_{3S1} are much larger than those of δ_{3D1} and ϵ_1 , which are almost negligible, we expect that the situation could be improved for strategy 2. Indeed, as one can see from Fig. 4 with the corresponding LECs

TABLE III: Values of the LECs of the best fit to the lattice QCD simulations of δ_{3S1} . The LECs in the first column are obtained by fitting to five lattice QCD data and those in the second column by fitting to six lattice QCD data.

$C_{3S1} [10^{-4} \text{ MeV}^{-2}]$	$\hat{C}_{3S1} [10^{-1} \text{ MeV}^{-2}]$	$\Lambda [\text{MeV}]$
0.669	-0.344	243
0.544	-0.559	231

given in Table IV, now δ_{3D1} and ϵ_1 are described reasonably well. However, δ_{3S1} are only in reasonable agreement with the lattice QCD data within the relatively large uncertainties of the lattice QCD simulations.

A particularly puzzling observation is that from $M_\pi = 138$ MeV to $M_\pi = 469$ MeV, the largest energy to which the leading order covariant ChEFT is applicable is reduced from about $T_{\text{lab.}} \approx 100$ MeV to about 10 MeV. This needs to be better understood in the future.

TABLE IV: Same as Table III, but fitted to δ_{3D1} and ϵ_1 .

$C_{3S1} [10^{-4} \text{ MeV}^{-2}]$	$\hat{C}_{3S1} [10^{-2} \text{ MeV}^{-2}]$	$\Lambda [\text{MeV}]$
0.207	0.780	548
0.260	0.825	513

B. Conventional ChEFT

In this section, we check how the physical and the lattice QCD nucleon-nucleon phase shifts can be described by the NLO conventional ChEFT. As noted earlier, in the conventional ChEFT, there are two LECs for the 3S_1 partial wave, one LEC for the mixing angle, and no LEC for the 3D_1 partial wave. As a result, the contribution to δ_{3D1} solely comes from the one-pion and two-pion exchanges. In this framework, the correlation between δ_{3S1} , δ_{3D1} , and ϵ_1 is induced by the one- and two-pion exchanges. We have checked that the two-pion

² The optimal cutoff values are a bit small compared to the preferred value of $0.5 \sim 1$ GeV, indicating that one should be less demanding in reproducing the lattice QCD data. On the other hand, as we can see in Table IV, the optimal cutoff values obtained by fitting to δ_{3D1} and ϵ_1 look more natural.

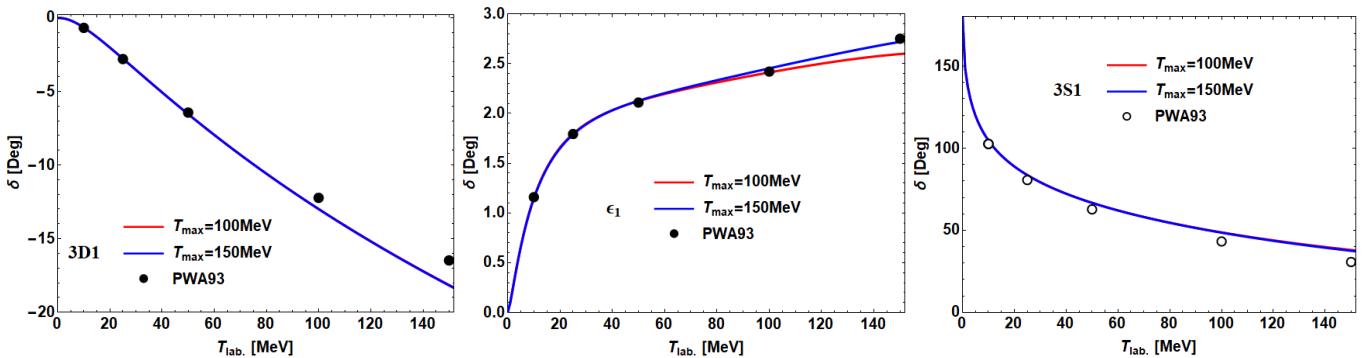


FIG. 2: Fitting to δ_{3D1} and ϵ_1 and predicting δ_{3S1} by the covariant ChEFT. Solid circles denote the data fitted and empty ones denote those not fitted.

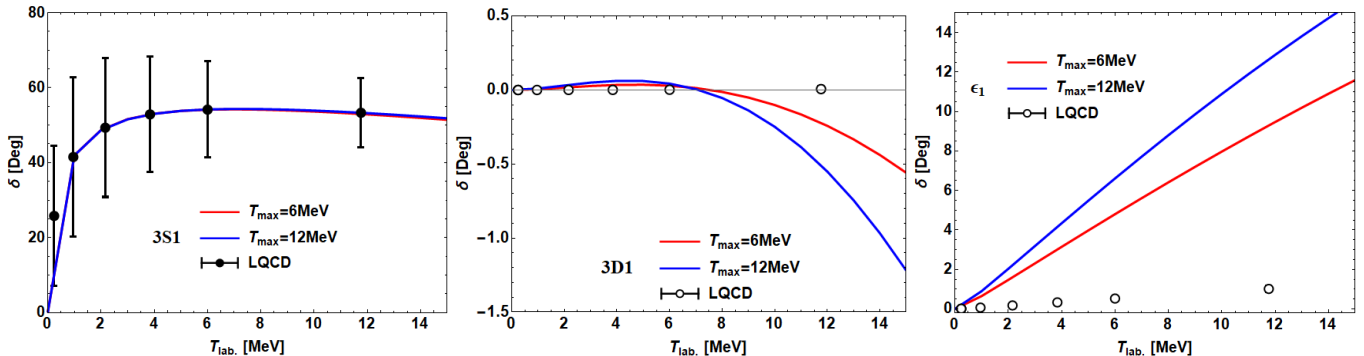


FIG. 3: Fitting to δ_{3S1} and predicting δ_{3D1} and ϵ_1 by the covariant ChEFT. Solid circles denote the data fitted and empty ones denote those not fitted.

exchange contributions are negligible. It should be noted that because the decoupling of LECs, we can only fit to δ_{3S1} , δ_{3D1} , and ϵ_1 simultaneously.

In Fig. 5, we compare the NLO conventional ChEFT results with the corresponding empirical data, with the LECs given in Table V. As can be clearly seen, up to $T_{\text{lab.}} \approx 100$ MeV, the empirical data can be described quite well, as already noted in Ref. [26], which is similar to the covariant ChEFT [26, 33]. In addition, the extra LEC for the mixing angle also allows for a better quantitative description of this observable.

Now we turn to the lattice QCD data obtained for $M_\pi = 469$ MeV. The corresponding results are shown in Fig. 6 and Table VI. One can see that the lattice QCD data can be described reasonably well only up to $T_{\text{lab.}} \approx 40$ MeV. Compared to the physical case, the energy range for which the NLO ChEFT works is also reduced by a factor of about three. Therefore, we can conclude that as the pion mass increases, the validity region of ChEFT in terms of kinetic energies for the nucleon-nucleon scattering is reduced.

IV. SUMMARY AND OUTLOOK

In this work, we explored the predictive power of the covariant chiral effective field theory for the nucleon-nucleon scattering in the 3S_1 - 3D_1 coupled channel, because the same

TABLE V: Values of the LECs of the best fit to the Nijmegen δ_{3S1} , δ_{3D1} , and ϵ_1 by the NLO conventional ChEFT.

C_{3S1P} [10^{-1} MeV $^{-2}$]	C_{3S1} [10^{-7} MeV $^{-4}$]	C_{3DS1} [10^{-8} MeV $^{-4}$]	Λ [MeV]
0.210	0.242	-0.557	662
0.251	0.254	-0.448	670

TABLE VI: Same as Table V, but fitted to the lattice QCD simulations by the NLO conventional ChEFT.

C_{3S1P} [10^{-1} MeV $^{-2}$]	C_{3S1} [10^{-7} MeV $^{-4}$]	C_{3DS1} [10^{-7} MeV $^{-4}$]	Λ [MeV]
0.115	0.235	-0.191	555
0.147	0.315	-0.195	540

low energy constants are responsible for the three observables δ_{3S1} , δ_{3D1} , and ϵ_1 . We checked the correlation using the physical NN phase shifts and found that it works pretty well up to $T_{\text{lab.}} \approx 100$ MeV. However, once applied to study the lattice QCD nucleon-nucleon phase shifts obtained for $M_\pi = 469$ MeV, we found that the covariant ChEFT only works up to $T_{\text{lab.}} \approx 10$ MeV at a quantitative level. Nevertheless, at a qualitative level, the correlation predicted by the covariant

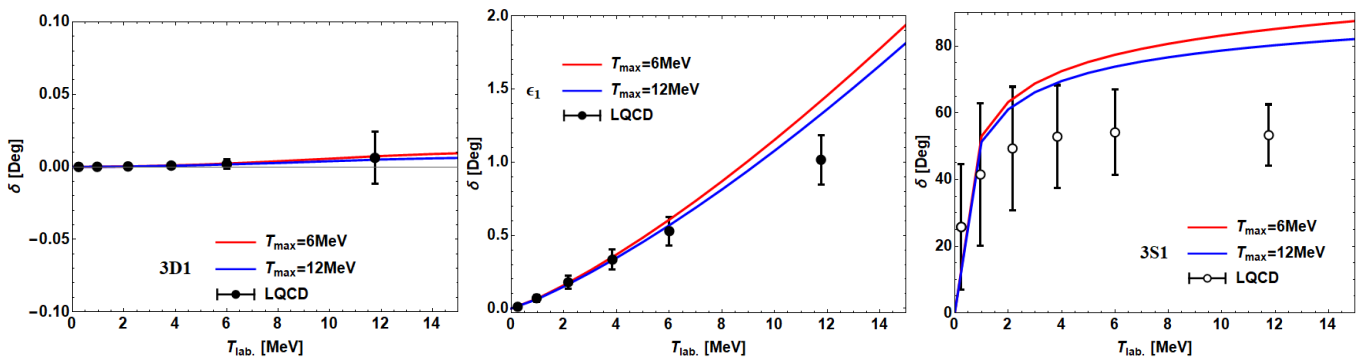


FIG. 4: Fitting to δ_{3D1} and ϵ_1 and predicting δ_{3S1} by the covariant ChEFT. Solid circles denote the data fitted and empty ones denote those not fitted.

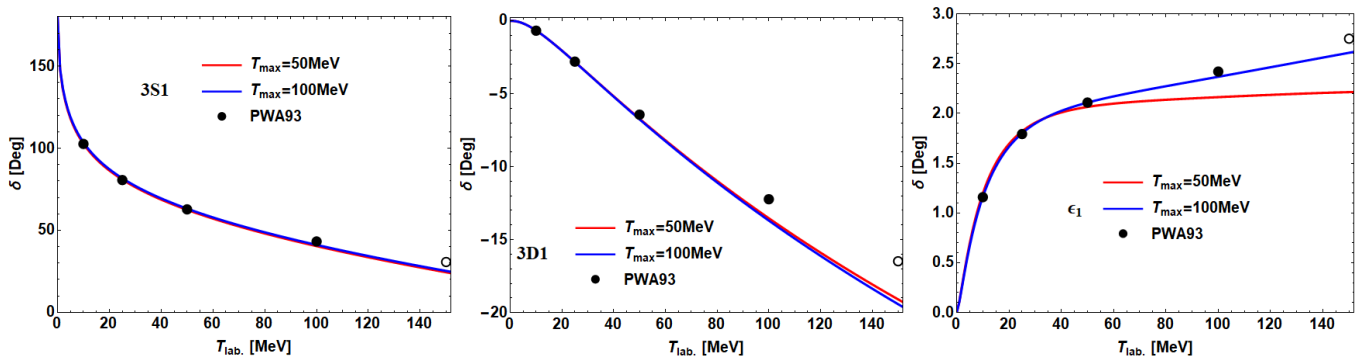


FIG. 5: Simultaneous description of the PWA93 phase shifts by the NLO conventional ChEFT.

ChEFT seems to hold for a larger kinetic energy.

To confirm the observed reduction of the validity region of ChEFT, we performed studies using the next-to-leading order conventional ChEFT. We found that with an additional independent LEC for the mixing angle ϵ_1 , the lattice QCD data can be reasonably described up to $T_{\text{lab.}} \approx 40$ MeV, which is larger than that of the leading order covariant ChEFT, but still roughly a factor of three smaller than the corresponding value achieved in describing the physical nucleon-nucleon phase shifts.

The correlation exhibited by the covariant ChEFT can be of relevance in understanding lattice QCD simulations of other baryon-baryon systems [28, 30, 34, 38], such as the strangeness $-3/ -4$ systems [34]. However, as the present study demonstrated, the validity region of ChEFT for unphysical pion masses might be considerably smaller than that for physical pion masses. This should be kept in mind when studying lattice QCD simulations obtained for large unphysical pion masses. In a recent work, it was shown that for the $\Lambda_c N$ system the lattice QCD data can only be described at a quantitative level up to $E_{c.m.} \approx 5$ MeV [39].

It should be noted that our current study is tied to the HALQCD simulations of the nucleon-nucleon interaction. It

will be of great value if other lattice QCD collaborations can perform more simulations, which may help better understand the pion mass dependence of the nucleon-nucleon interaction, and baryon-baryon interactions in general. In recent years, a large amount of the-called exotic hadrons, which cannot easily fit into the conventional quark model, have been discovered at world-wide high energy facilities, such as LHC, KEKB, and BEPC. Because many of them are located close to the thresholds of two conventional hadrons, they are believed to be hadronic molecules. Clearly, in such a picture, lattice QCD simulations of hadron-hadron interactions are very important to understand these exotic hadrons. Our current work could also be of relevance to such studies.

V. ACKNOWLEDGEMENTS

This work is partly supported by the National Natural Science Foundation of China under Grants No.11735003, No.11975041, and No.11961141004, and the fundamental Research Funds for the Central Universities.

[1] S. Aoki and T. Doi, *Front. in Phys.* **8**, 307 (2020), 2003.10730.

[2] M. Illa et al. (NPLQCD), *Phys. Rev. D* **103**, 054508 (2021),

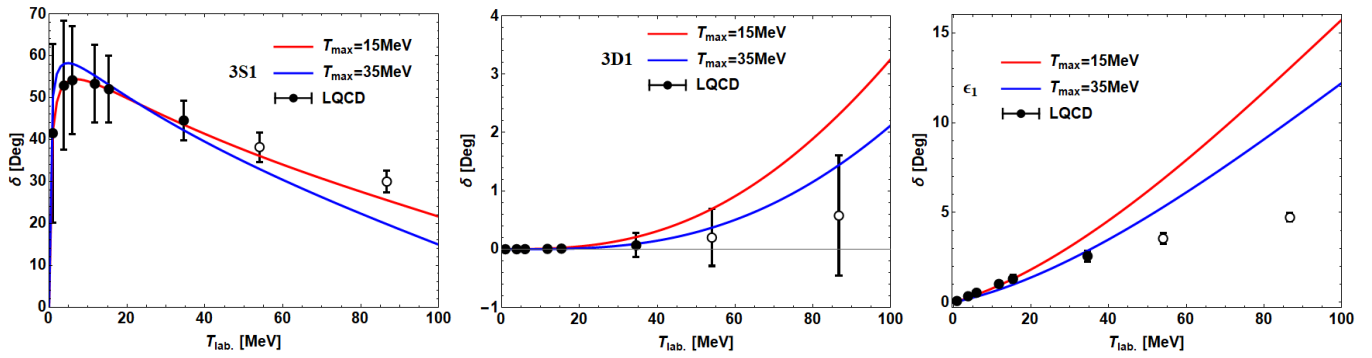


FIG. 6: Simultaneous description of the HALQCD469 phase shifts by the NLO conventional ChEFT.

- 2009.12357.
- [3] M. L. Wagman, F. Winter, E. Chang, Z. Davoudi, W. Detmold, K. Orginos, M. J. Savage, and P. E. Shanahan, *Phys. Rev. D* **96**, 114510 (2017), 1706.06550.
- [4] T. Inoue, N. Ishii, S. Aoki, T. Doi, T. Hatsuda, Y. Ikeda, K. Murano, H. Nemura, and K. Sasaki (HAL QCD), *Phys. Rev. Lett.* **106**, 162002 (2011), 1012.5928.
- [5] S. R. Beane et al. (NPLQCD), *Phys. Rev. Lett.* **106**, 162001 (2011), 1012.3812.
- [6] N. Ishii, S. Aoki, and T. Hatsuda, *Phys. Rev. Lett.* **99**, 022001 (2007), nucl-th/0611096.
- [7] R. A. Briceño, Z. Davoudi, T. Luu, and M. J. Savage, *Phys. Rev. D* **88**, 114507 (2013), 1309.3556.
- [8] K. Sasaki et al. (HAL QCD), *Nucl. Phys. A* **998**, 121737 (2020), 1912.08630.
- [9] S. Weinberg, *Physica A* **96**, 327 (1979).
- [10] J. Gasser and H. Leutwyler, *Annals Phys.* **158**, 142 (1984).
- [11] J. Gasser, M. E. Sainio, and A. Svarc, *Nucl. Phys. B* **307**, 779 (1988).
- [12] S. Scherer and M. R. Schindler, *A Primer for Chiral Perturbation Theory*, vol. 830 (2012), ISBN 978-3-642-19253-1.
- [13] S. Weinberg, *Phys. Lett.* **B251**, 288 (1990).
- [14] S. Weinberg, *Nucl. Phys.* **B363**, 3 (1991).
- [15] C. Ordonez, L. Ray, and U. van Kolck, *Phys. Rev. C* **53**, 2086 (1996), hep-ph/9511380.
- [16] P. F. Bedaque and U. van Kolck, *Ann. Rev. Nucl. Part. Sci.* **52**, 339 (2002), nucl-th/0203055.
- [17] E. Epelbaum, H.-W. Hammer, and U.-G. Meißner, *Rev. Mod. Phys.* **81**, 1773 (2009), 0811.1338.
- [18] R. Machleidt and D. R. Entem, *Phys. Rept.* **503**, 1 (2011), 1105.2919.
- [19] E. E. Jenkins and A. V. Manohar, *Phys. Lett. B* **255**, 558 (1991).
- [20] V. Bernard, N. Kaiser, J. Kambor, and U. G. Meißner, *Nucl. Phys. B* **388**, 315 (1992).
- [21] T. Fuchs, J. Gegelia, G. Japaridze, and S. Scherer, *Phys. Rev. D* **68**, 056005 (2003), hep-ph/0302117.
- [22] L. Geng, *Front. Phys. (Beijing)* **8**, 328 (2013), 1301.6815.
- [23] E. Epelbaum and J. Gegelia, *Phys. Lett. B* **716**, 338 (2012), 1207.2420.
- [24] V. Baru, E. Epelbaum, J. Gegelia, and X. L. Ren, *Phys. Lett. B* **798**, 134987 (2019), 1905.02116.
- [25] X. L. Ren, E. Epelbaum, and J. Gegelia, *Phys. Rev. C* **101**, 034001 (2020), 1911.05616.
- [26] X.-L. Ren, K.-W. Li, L.-S. Geng, B.-W. Long, P. Ring, and J. Meng, *Chin. Phys.* **C42**, 014103 (2018), 1611.08475.
- [27] K.-W. Li, X.-L. Ren, L.-S. Geng, and B.-W. Long, *Chin. Phys.* **C42**, 014105 (2018), 1612.08482.
- [28] K.-W. Li, T. Hyodo, and L.-S. Geng, *Phys. Rev. C* **98**, 065203 (2018), 1809.03199.
- [29] Y. Xiao, L.-S. Geng, and X.-L. Ren, *Phys. Rev.* **C99**, 024004 (2019), 1812.03005.
- [30] J. Song, K.-W. Li, and L.-S. Geng, *Phys. Rev. C* **97**, 065201 (2018), 1802.04433.
- [31] Y. Xiao, C.-X. Wang, J.-X. Lu, and L.-S. Geng, *Phys. Rev. C* **102**, 054001 (2020), 2007.13675.
- [32] Q.-Q. Bai, C.-X. Wang, Y. Xiao, and L.-S. Geng, *Phys. Lett. B*, 135745 (2020), 2007.01638.
- [33] C.-X. Wang, L.-S. Geng, and B. Long, *Chin. Phys. C* **45**, 054101 (2021), 2001.08483.
- [34] Z.-W. Liu, J. Song, K.-W. Li, and L.-S. Geng, *Phys. Rev. C* **103**, 025201 (2021), 2011.05510.
- [35] T. Inoue, S. Aoki, T. Doi, T. Hatsuda, Y. Ikeda, N. Ishii, K. Murano, H. Nemura, and K. Sasaki (HAL QCD), *Nucl. Phys. A* **881**, 28 (2012), 1112.5926.
- [36] E. Epelbaum, H. Krebs, and U. G. Meißner, *Eur. Phys. J. A* **51**, 53 (2015), 1412.0142.
- [37] J. Haidenbauer and G. Krein, *Eur. Phys. J. A* **54**, 199 (2018), 1711.06470.
- [38] J. Song, Y. Xiao, Z.-W. Liu, C.-X. Wang, K.-W. Li, and L.-S. Geng, *Phys. Rev. C* **102**, 065208 (2020), 2010.06916.
- [39] J. Song, Y. Xiao, Z.-W. Liu, K.-W. Li, and L.-S. Geng (2021), 2104.02380.
- [40] J. Hu, Y. Zhang, H. Shen, and H. Toki, *Chin. Phys. C* **44**, 071002 (2020), 2003.08008.